Quantitative Measurements of Force and Displacement Using an Optical Trap

Robert M. Simmons,* Jeffrey T. Finer,‡ Steven Chu,§ and James A. Spudich‡
*MRC Muscle and Cell Motility Unit, Randall Institute, King's College London, London WC2B 5RL, England; ‡Departments of Biochemistry and Developmental Biology, Beckman Center, Stanford University Medical Center, and §Department of Physics, Stanford University, Stanford, California 94305 USA

ABSTRACT We combined a single-beam gradient optical trap with a high-resolution photodiode position detector to show that an optical trap can be used to make quantitative measurements of nanometer displacements and piconewton forces with millisecond resolution. When an external force is applied to a micron-sized bead held by an optical trap, the bead is displaced from the center of the trap by an amount proportional to the applied force. When the applied force is changed rapidly, the rise time of the displacement is on the millisecond time scale, and thus a trapped bead can be used as a force transducer. The performance can be enhanced by a feedback circuit so that the position of the trap moves by means of acousto-optic modulators to exert a force equal and opposite to the external force applied to the bead. In this case the position of the trap can be used to measure the applied force. We consider parameters of the trapped bead such as stiffness and response time as a function of bead diameter and laser beam power and compare the results with recent ray-optic calculations.

INTRODUCTION

In a single-beam gradient optical trap, or optical tweezers, a laser beam is brought to a focus in an aqueous solution by a high numerical aperture microscope objective (Ashkin et al., 1986). Any refractile particle near the focus is attracted to it and becomes trapped. The method has been used in a number of biological applications both as a micromanipulator and as a force transducer. Cells, organelles, and chromosomes can be directly manipulated, whereas measurements of the magnitudes of the forces between proteins such as molecular motors require the proteins to be attached to trapped silica or polystyrene beads (see reviews: Block, 1990; Berns et al., 1991; Kuo and Sheetz, 1992; Simmons and Finer, 1993). The trapping force is of the order of 1–100 pN, depending upon the size and refractive index of the particle and the power and wavelength of the laser beam.

Initial attempts to use optical traps as force transducers involved measurement of the applied force necessary to cause the particle to escape the optical trap. This method gives an estimate of the peak force, but it is unable to measure fluctuations in the applied force. More recently, we and others have detected the position of a trapped particle and used it to measure force (Simmons et al., 1993; Kuo and Sheetz, 1993; Svoboda et al., 1993; Finer et al., 1994). In this paper we describe the full details and justification of our method, combining an optical trap with a high-resolution position detector to show that when a force is applied to a trapped bead, the bead is displaced from the center of the trap by an distance that is proportional to the applied force. When the applied force is changed rapidly, the rise time of the bead displacement is on the millisecond time scale, and thus a trapped bead can be used as a transducer of force fluctuations. We consider parameters of the trapped bead such as stiffness and response time as a function of bead diameter, bead position within the trap, and laser beam power, and compare the results with recent ray-optic calculations of the forces on trapped beads (Ashkin, 1992).

Finally, we show that the performance of an optical trap as a force transducer can be enhanced by means of a feedback circuit. As an external force is applied to a trapped bead, the position of the trap moves to exert an equal and opposite force on the bead. Ashkin and Dziedzic (1977) used feedback to stabilize the vertical (z) position of a particle levitated by a laser beam in a vacuum by modulating the laser beam intensity. In contrast, in our system the feedback is applied to a gradient optical trap in the plane perpendicular to the beam axis using acousto-optic deflectors to shift the trap position rapidly. As a result, the stiffness of the trap is greatly increased, so that the bead is held stationary with nanometer precision, and the position of the trap can be used to measure applied force fluctuations.

MATERIALS AND METHODS

Optics

The apparatus is a modification and extension of an optical trap microscope designed by Chu, Kron, and Sunderman (unpublished). In Fig. 1, the original apparatus consisted of the Nd-YAG laser, mirrors M_1 and M_2 used for steering the laser beam manually, the collimating lens L_2, and a microscope (Zeiss Axioplan). The microscope was modified to accept the laser beam by cutting a hole in the side and inserting a dichroic mirror in place of the eyepiece prisms. The parallel laser beam entered the back aperture of the microscope objective (Zeiss Plan-Neofluar 63×, 1.25 NA, infinity corrected, oil immersion) and was brought to a focus at the specimen, forming the optical trap. A major principle of the optical system

Received for publication 29 December 1995 and in final form 10 January 1996.

Address reprint requests to Dr. James A. Spudich, Department of Biochemistry, Stanford University School of Medicine, Beckman Center, Stanford, CA 94305-5307.

0006-3495/96/04/1813/10 $2.00

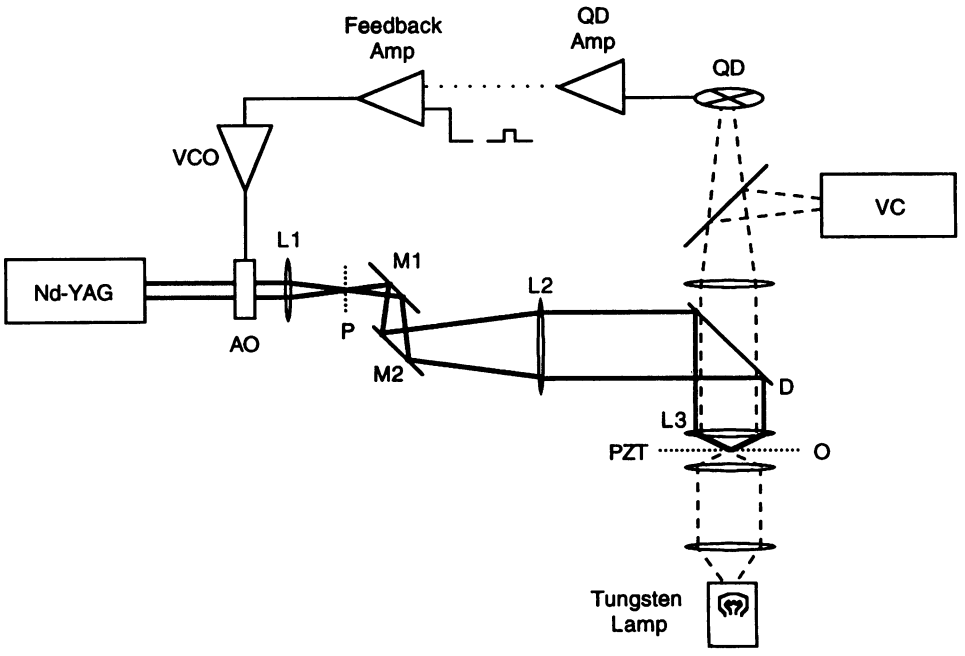

FIGURE 1 Schematic diagram of the optical trap and detection system. The solid lines represent the path of the Nd-YAG laser. The dashed lines represent the illuminating light from a tungsten lamp. Optics include lenses (L_1, L_2), mirrors (M_1, M_2), a dichroic filter (D), and a microscope objective (L_3). The laser beam can be shifted in the plane of the specimen (O) by deflecting it with two orthogonally mounted acousto-optic modulators (AO) and by moving the mirrors M_1, M_2. The illuminating light is split between a video camera (VC) and a quadrant photodiode detector (QD), which indicates the position of a trapped bead. The feedback loops can be closed by feeding the output signals from the quadrant detector into the driver circuits for the voltage-controlled oscillators (VCO), which control the acousto-optic modulators.

was that the lens L_2 collimated an expanding laser beam at its front focal point, turning it into a parallel beam that just filled the back aperture of the microscope objective, L_3, at its other focal point. A lateral movement of one of the mirrors M_1, M_2 shifted the laser beam parallel to the axis, so that the beam entered the objective at an altered angle to the optical axis. This resulted in a lateral shift in the position of the focal spot. The beam still filled the back aperture of the objective, so the strength of the trap remained roughly constant for displacements of up to 50 μm off-axis. The plane, P, containing the real or apparent point of divergence of the laser beam, was conjugate to the objective focal plane, O. A lateral movement of one of the mirrors M_1, M_2 produced an equal shift of the apparent point source in plane P, and the corresponding movement in plane O was a factor of f_2/f_3 smaller. f_2 was 400 mm and f_3 about 3 mm, so f_2/f_3 was about 150. In experiments in which two beads were to be trapped, the beam was split before it reached mirror M_1, using a half-waveplate followed by a polarizing beam splitter (not shown in Fig. 1). The second pathway also had a pair of mirrors, and the two beams were brought together with a second polarizing beam splitter before lens L_2.

We made the following additions to the apparatus. In some of our experiments (e.g., Finer et al., 1994) it is necessary to move the positions of the traps rapidly under manual control, so we motorized the mirror movements and operated them with a joystick control (Newport positioners 860A-1-HS, controller 860-C2). For fast, electronically controlled movements of the traps, we added two acousto-optic modulators, placed orthogonally (AO_1, AO_2; Isomet 1206C with D323B drivers). An additional lens, L_1, was placed so that the midpoint of AO_1 and AO_2 lay at one focus, and the focal point of L_2 at the other. AO_1 and AO_2 acted as diffraction gratings whose spacings were determined by an acoustical wave of variable frequency. They were set relative to the incident beam at the Bragg angle for the first-order diffracted beam to maximize the intensity in the first-order beam. A change of frequency, resulting from a change in the input voltage to the driver, produced a change in the diffraction angle. The useful range (over which the intensity of the diffracted beam did not vary by more than $\pm$10%) was about 12 mradians. The deflection response of an acousto-optic modulator was measured separately; for this measurement the output diffracted laser beam was focused onto a quadrant detector. The response to a square wave input showed a lag of about 4 μs followed by a rise that was 90% complete in 9 μs. Peak-to-peak positional noise was about 10^{-4} of the maximum deflection.

The function of L_1 was to convert an angular deflection from the acousto-optic modulators into a lateral shift of the laser beam parallel to the optical axis. For a deflection θ, the lateral shift of the beam at plane P was $f_1 \cdot \theta$, and at plane O it was $(f_1 \cdot f_3/f_2) \cdot \theta$. f_1 was determined by the magnification required for the width of the laser beam to fill the back aperture of the objective, as follows. The beam waist at the acousto-optic modulators was about 1 mm; this was necessary for optimal beam quality and was produced using a telescope at the laser. The objective back aperture was 7 mm wide, so the magnification had to be 7. The magnification is given by f_2/f_1, so f_1 had to be 60 mm. The factor $(f_1 \cdot f_3/f_2)$ was then about 400 nm $\cdot$ mradian^{-1}. The total useful movement of the trap using an acousto-optic modulator was about 4 μm. The acousto-optic modulators noticeably degraded the quality of the beam and required careful adjustment to optimize the strength of the laser trap. Slightly different settings could produce changes of trap strength differing by a factor of up to 4. At optimal adjustment the efficiency of each modulator was only about 30–40%. Coupled with a restriction on laser power at entry to the acousto-optic modulators of 1 W, the maximum power available at the objective was about 0.2 W.

The laser used in these experiments (Quantronix 416, 10 W Nd-YAG, 1.064 μm) was stable only at laser powers in excess of 5 W. We attenuated the beam immediately after the laser with a half-waveplate and polarizing beam splitter. For finer variations of intensity we used a variable attenuator (Newport 925B) inserted beyond the acousto-optic modulators. An alternative method was to vary the power input to the acousto-optic modulators, but in practice this method was not used much, as it caused an appreciable movement of the beam. The power of the beam entering the microscope was measured from the intensity of the radiation reflected from an optical surface and focused onto a power meter (Coherent Fieldmaster). About half the power would be expected to be lost in the objective (Svoboda and Block, 1994).

Illumination of the specimen was by conventional transmitted light, using a 100-W tungsten lamp with a DC power supply. Illumination for epifluorescence was by a 100-W mercury arc lamp. Light emerging from the microscope was split between a videocamera (VC) and a quadrant photodiode detector (QD) to monitor the bead position, using a beam splitter with selectable ratios (Zeiss 473051). Images of the specimen were projected onto the front surfaces of the video camera and the quadrant detector using eyepieces, 10$\times$ in the case of the videocamera and between 7$\times$ and 20$\times$ with auxiliary singlet lenses as necessary for the quadrant detector, depending on the size of bead in use. The image of the bead filled approximately half the area of the quadrant detector. The distances of the

camera and the quadrant detector from the eyepieces could be adjusted to give satisfactory magnifications.

The specimen was viewed using a SIT camera (Hamamatsu C2400–08) with either brightfield or fluorescent illumination, followed by an image-processing system (Hamamatsu Argus 10). The videocamera output was digitized with a frame grabber (Data Translation DT2855) interfaced to a personal computer, and the positions of the mirrors M_1–M_4 were monitored and superimposed on the video image as cursors showing the positions of the traps. The mirror positions were derived using voltage dividers consisting of spring-loaded potentiometers attached to the stage movements. The voltages were read into the computer by analog-to-digital converters (Data Translation DT2814). The focusing of the video camera image could be adjusted by a motorized movement based on a 35-mm camera lens focusing movement, so as to have an independent control over focus. This was necessary because the normal focusing controls of the microscope altered the z-position of the trap as well as the optical focus.

The brightfield image of a bead projected onto the quadrant detector was deliberately defocused so as to enhance the contrast between the bead and the background. This was done by moving the eyepiece away from its normal focus position, so that the image appeared dark on a bright background. Contrast was further enhanced by closing the condenser diaphragm. Adjustments were in general made to optimize the signal while the position of the trap was moved with a square wave (see below).

The whole apparatus was mounted on an antivibration table (Newport). However, there were a number of sources of instrumental noise that affected the measurements. The attachments to the microscope, which was of upright design, introduced a number of low-frequency vibrations, which were excited by the flow of cooling water to the laser. These were substantially reduced, but not eliminated, by surrounding the vertical column extending from the body of the microscope to the quadrant detector and video camera with a metal box filled with lead shot. Pointing instability in the laser and in the laser beam path, which in these experiments was not enclosed, also contributed noise, chiefly drift. Signal averaging was used to estimate the time constant of trapped beads and movement in response to external forces, and this greatly reduced the effect of noise from these sources and from Brownian motion.

Electronics

The x and y coordinates of a trapped bead (x_B, y_B) were determined using a quadrant photodiode detector (Hamamatsu S4349), chosen for its small active area. This minimized dark noise (which is in part proportional to photodiode area) and reduced the amount of magnification needed, leading to a more compact design that was less prone to vibration. The amplifier circuit (Fig. 2 *B*) used low-noise current-to-voltage converters and had switched feedback resistors (omitted from Fig. 2 *B*), which could be selected to maximize the output. x_B and y_B were obtained by appropriate subtractions and additions of the signals. The quadrant detector was mounted on a manual XY movement controlled by micrometers. There was some variation in background illumination over the field at the quadrant detector, which was therefore moved to a point where the background was flat. For most of the measurements in this paper we used 10-MΩ feedback resistors in the quadrant detector, which gave a bandwidth of 2 kHz, measured from the response of the quadrant detector to a light from an LED with a square wave voltage input. Signals were averaged to reduce the noise from Brownian motion and other sources. For measurements where signal averaging was not possible (e.g., when recording Brownian motion) and where it was necessary to maximize the signal relative to instrumental noise, we used 200-MΩ resistors, giving a bandwidth of 100 Hz.

A feedback circuit was designed and built to increase the stiffness of the trap (Fig. 2 *C*). This consisted of integrating and direct pathways for the x_B and y_B signals, and the outputs of the circuit were fed to the drivers for AO_1 and AO_2, with appropriate offsets to produce steady deflections of the laser beam. The operation of the feedback circuit was controlled by analog switches S_1, S_2. In some circumstances, such as when an external force was acting on a trapped bead, the bead position could be far from zero, and when the feedback was switched on, there was a rapid transient as the servo loop acted to return the bead to its central position. This was minimized by the use of sample-and-hold circuits, as shown in Fig. 2 *A*, to zero the x_B and y_B signals just before the feedback was switched on, so that the bead remained at its offset position.

To a good approximation, movements of the trap position could be regarded as being linear and instantaneous on the time scale of the measurements made in this work. Thus, the trap position (x_T, y_T) could be obtained from the input voltages to the drivers of the acousto-optic modulators. For the present study, the force acting on a bead could be obtained from the x_B, y_B or x_T, y_T signals as appropriate. However, for more general applications we designed further electronic circuits to calculate F_x and F_y, the x and y components of external force acting on a bead, from the difference between the bead position and the position of the trap. An allowance was made for the viscous drag of the solution acting on the bead when it moves, as follows:

$$F_x = k_T(x_T - x_B) - b\frac{dx_B}{dt}$$

$$F_y = k_T(y_T - y_B) - b\frac{dy_B}{dt},$$

where k_T is the stiffness of the trap and b is the damping factor.

Force calibration

Calibration for force was performed by flowing solution past a trapped bead at a known velocity and calculating the force from Stokes' law,

$$F = 6\pi\eta r v,$$

where v is the velocity, r is the radius of the bead, and η is the viscosity of the solution. This was done by moving a microscope substage, consisting of a carrier for a microscope slide, by means of two piezoelectric transducers (PZTs) (Physik Instrumente P771) attached to the stage of the microscope. The PZTs had a natural frequency of about 500 Hz and total range of about 50 μm. They were also used in certain motility assay experiments to track a moving bead by moving the substage and were controlled for this purpose by a joystick. The movement of the stage (usually 5 μm) in response to the triangular wave input used in the calibration procedure was recorded separately, using a low-power objective to project the image of an opaque object onto the quadrant detector. Measurements and calibrations were all done with the trapped bead about 5 μm below the surface of the coverslip, where surface perturbations of Stokes' law should be negligible (Happel and Brenner, 1991; Svoboda and Block, 1994). The trapping force was only slightly lower than at the surface.

Data recording

The x_B, y_B, x_T, and y_T signals were digitized using an analog-digital converter (RC Electronics, ISC-16) interfaced to a personal computer, sampling at rates up to 250 kHz, depending on the bandwidth of the data, and stored on magnetic disk.

Inverted microscope

The records in this paper, with the exception of those in Fig. 12, were obtained using the modified vertical microscope system described in the sections above. We subsequently improved this system in two stages. In the first stage, we built an inverted microscope configuration with improvements in positional stability and with decreased instrumental noise, mainly resulting from substituting a xenon lamp for the tungsten lamp (Finer et al., 1994). Otherwise the optics and electronics were similar to those described above. In the second stage we improved the bandwidth of the detector when using a 100-MΩ resistor to 5 kHz, by the use of a correction circuit

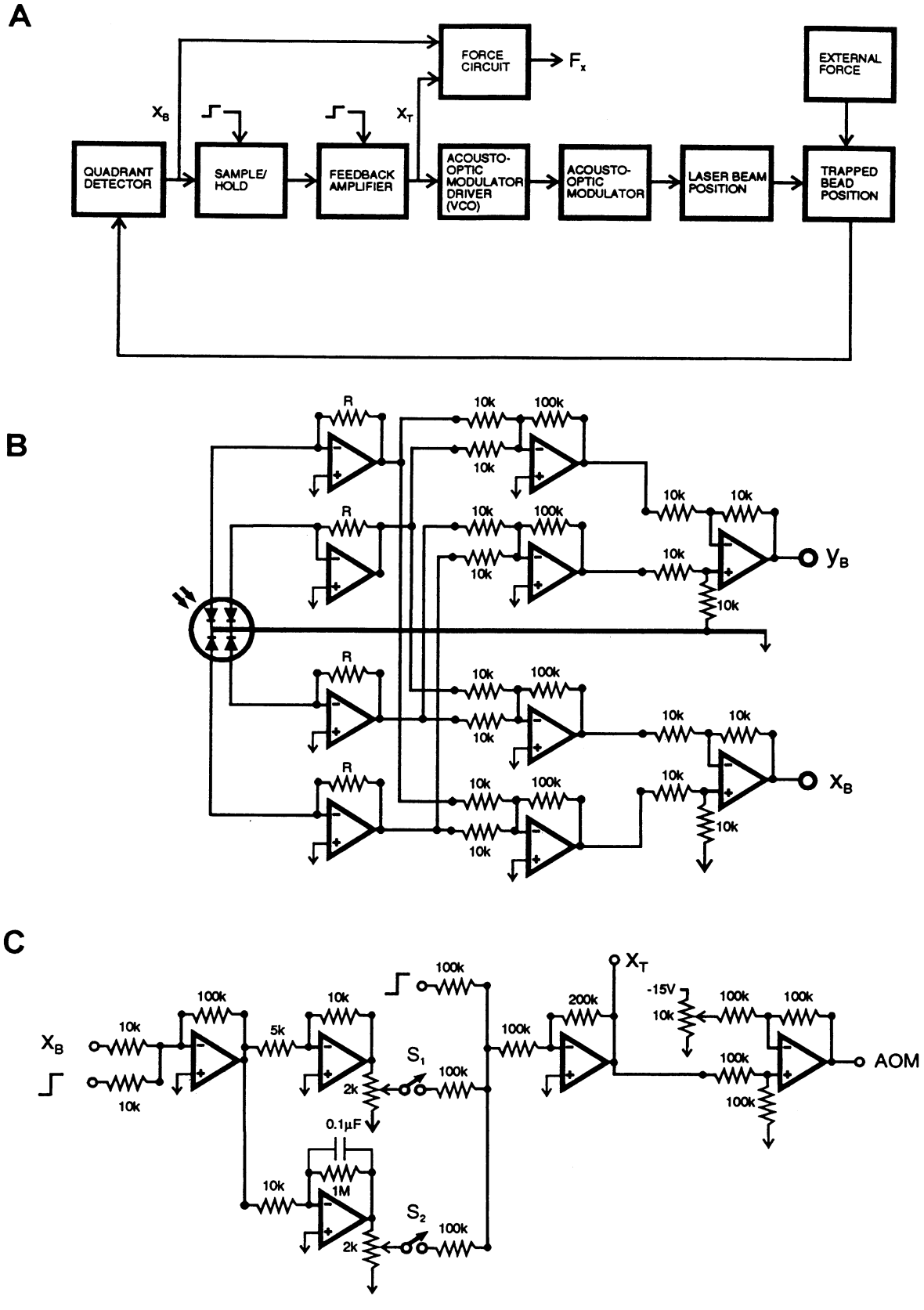

FIGURE 2 (*A*) Block diagram of one channel of electronic circuits showing feedback arrangements. The pulse inputs were used to open and close the feedback loop. (*B*) Quadrant detector circuit. The feedback resistors *R* had a switched range, 10 kΩ to 200 MΩ. Operational amplifiers: first stage, OPA121; second stage, OP270; final stage, AMP03. (*C*) Feedback amplifier circuit (one channel). Operational amplifiers: OP27. S_1, S_2; analog switches used to open and close the feedback loop. Pulse inputs were used to deflect the laser beam.

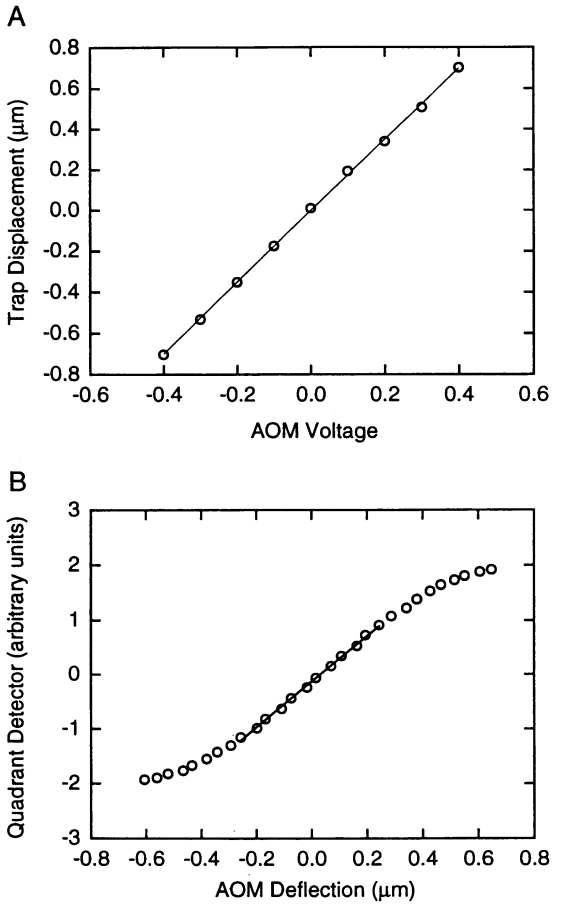

FIGURE 3 (*A*) Acousto-optic modulator (AOM) calibration. There is a linear relation between the input voltage to the AOM and the trap position over the 1.5-μm range shown. (*B*) Quadrant photodiode detector calibration. The AOM deflection represents the bead position. The line shows the linear range of the quadrant detector for bead displacements of 0.2 μm away from the center in each direction.

incorporating a differentiator. The performance of the feedback system was also improved, by incorporating a differential pathway in parallel with the direct and integrating pathways shown in Fig. 2 *C*. The records in Fig. 12 were obtained using the final modifications.

RESULTS

Measurements on 1-μm diameter beads

The majority of our detailed measurements were made on 1-μm beads, which is the diameter used in our experiments on the actomyosin motility assay (Simmons et al., 1993; Finer et al., 1994). We first calibrated the microscope magnification using a stage micrometer, whose image was projected onto the quadrant detector. The distance between successive 10-μm rulings was found by moving the micrometers controlling the position of the detector. Using a trapped bead of 1 μm diameter, we next calibrated AO_1 and AO_2 by applying a square wave to the output stage amplifiers in the feedback circuit (Fig. 2) to move the position of the trap, and measuring on an oscilloscope the movement of the micrometers necessary to null the resulting signal from the quadrant detector (Fig. 3 *A*). Applying a slow triangular wave, we then calibrated the quadrant detector (Fig. 3 *B*). The output was roughly sinusoidal with respect to bead displacement, and for the measurements reported here we kept within the range of movements for which the output of the detector did not depart from linearity by greater than 5%. We refer to this as the linear range of the quadrant detector. In some cases we corrected the responses for the nonlinearity of the detector, but the effect on the results was negligible.

When the position of the trap was moved by applying a square wave input to one of the acousto-optic modulators, a trapped bead followed the movement of the beam with a lag that was nearly first-order for small steps (Fig. 4 *A*). This result shows that a trapped bead behaves as a damped mass in a parabolic energy well, i.e., as if it were attached to the center of the trap by a spring. Calculations using the observed stiffness confirm that the trapped bead can be described as a harmonic oscillator that is so highly damped

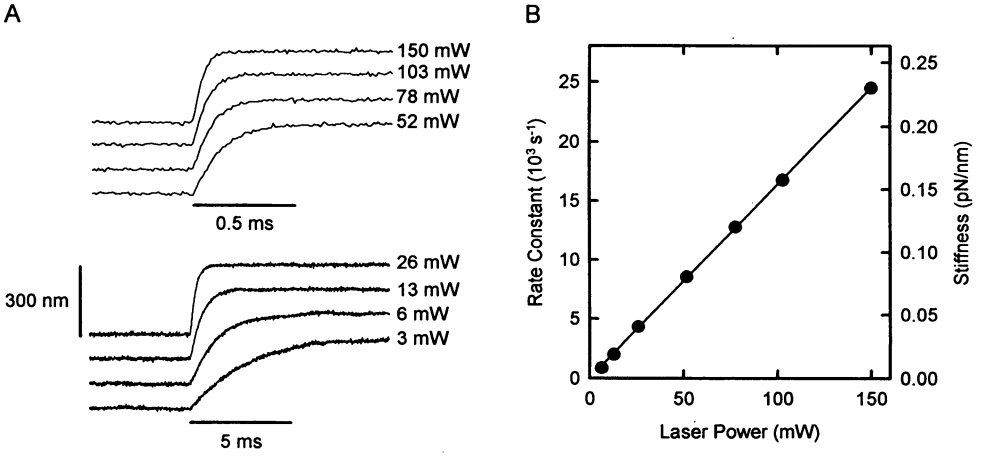

FIGURE 4 (*A*) Response of a trapped bead (1-μm diameter) to rapid trap displacements of 300 nm at laser powers ranging from 3 to 150 mW. For laser powers of 52 to 150 mW the response is shown on an expanded time scale. Detector bandwidth was 20 kHz (single-pole, low-pass filter). Each trace is an average of 100 data sweeps. (*B*) The rate constant of the bead response as a function of laser power.

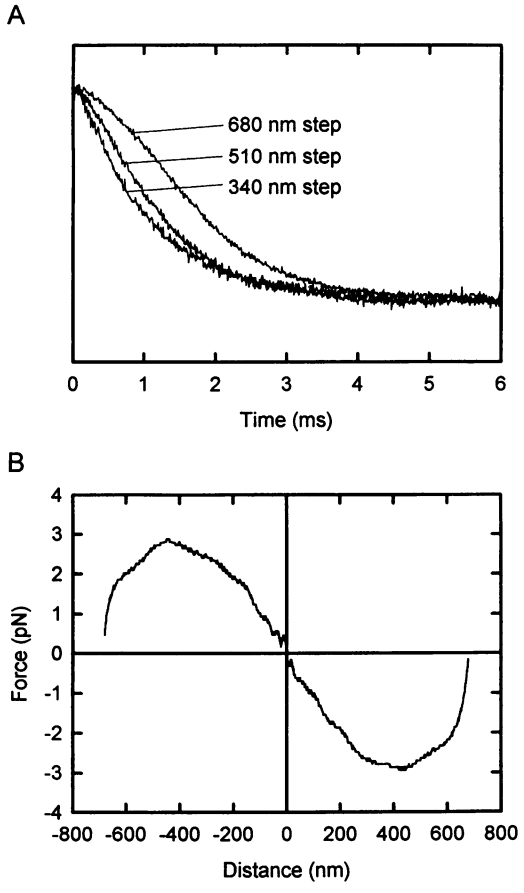

FIGURE 5 (*A*) Time course of the response of a trapped 1-μm-diameter bead for rapid trap displacements of 340, 510, and 680 nm. The responses are normalized to fit on the same scale to illustrate the lag in the response for large trap displacements. Detector bandwidth was 20 kHz (single-pole, low-pass filter). Each trace is an average of 100 data sweeps. (*B*) Force profile of an optical trap as a function of displacement of a bead from the center of the trap. The force was calculated by differentiating the bead response to a large trap displacement and calculating the viscous (Stokes') force.

that the inertial term in the equation of motion can be neglected, so that the movement of the bead after a sudden trap displacement is given by

$$x_B = x_T(1 - e^{-(k/b)t}),$$

where k is the stiffness of the trap and b is the damping factor. The stiffness depends on the laser power, the size of bead, and its refractive index, and on other factors such as the numerical aperture of the objective (Ashkin, 1992). The dependence of the rate constant, k/b, on laser beam power for 1-μm-diameter beads is shown in Fig. 4 *B* for the range 3–150 mW. The rate constant varied linearly from 800 s^{-1} for 5 mW to 25,000 s^{-1} for 150 mW. The value of k can be derived by calculating b from Stokes' law (see Materials and Methods); k is shown in Fig. 4 *B*. It varied from 0.007 to 0.23 pN/nm over the range measured.

The time course of bead movement was independent of the amplitude up to a certain limit, but beyond this there was an increasing lag of the response with increase of step size (Fig. 5 *A*). This was shown to result from a fall in the force as the trap was offset. The profile of force across the trap was calculated from a record for a large step, by taking the derivative of the response (Fig. 5 *B*) and plotting it against displacement. The curve shows that, as the trap is displaced from the center of the bead, force changes at first approximately linearly and then reaches a broad peak at about 450 nm, after which it falls off more steeply, so that the total half-width of the trap is about 675 nm. This confirms the calculation by Ashkin (1992) that the maximum force should be reached when the trap is at about the radius of the bead, although his calculation is strictly applicable only to much larger beads.

Another method of exploring the profile of the energy well and obtaining the value of the trap stiffness is to apply an external force to a trapped bead and measure the resulting displacement. This has the advantage that external forces can be applied over a much longer time, and the true steady-state values of displacement can be measured. We did this by applying triangular waves of varying velocity and amplitude to the PZT-controlled microscope substage (Fig. 6 *A*). The movement of the substage was first recorded by projecting onto the quadrant detector the image of a small opaque object on a microscope slide attached to the substage, using a low-power objective. The movement of the PZTs was slightly nonlinear, but it was found that the average velocity of movement was negligibly different from the velocity calculated from the total excursion and the

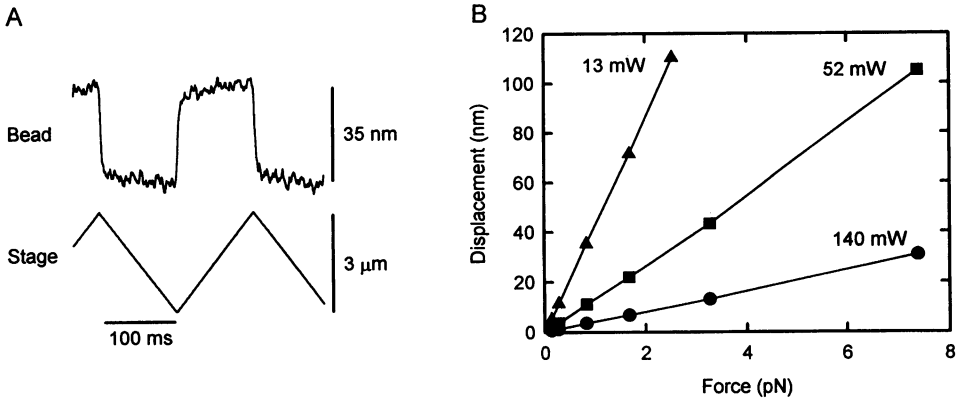

FIGURE 6 (*A*) The response of a trapped bead to a triangular wave input to the microscope stage position. The bead shows a square wave response corresponding to the viscous force. Detector bandwidth was 100 Hz (single-pole, low-pass filter). Each trace is an average of 100 data sweeps. (*B*) Displacement of a bead from the center of the trap as a function of the applied viscous force for 13, 52, and 140 mW laser powers.

duration. We then measured the average displacement of a trapped bead as a function of Stokes' force. Fig. 6 *B* shows that the steady displacement was linearly related to the applied force, making the important point that the movement of the bead in the trap can be used as a force transducer in the piconewton and sub-piconewton force range. Using long periods of signal averaging to remove noise arising from Brownian motion and other sources, we found that the relationship holds down to the smallest force applied, 0.14 pN.

These measurements gave direct values of trap stiffness that were in good agreement with those estimated from the time constant of displacements produced by the acousto-optic modulators. The force applied in these tests approximated to a square wave, and the resulting displacement had a time constant that is similar to that measured using the acousto-optic modulators under the same conditions. However, the movement produced by the piezoelectric transducers was much slower than that produced by the acousto-optic modulators, and we did not attempt to make any quantitative measurements of rise time using this method.

A method used to measure the force on trapped particles or beads in biological experiments is to estimate the "escape force." As already shown in Fig. 5 *B*, force rises to a maximum with displacement of a trapped bead and then falls off again. So if a force is applied that just exceeds the maximum that the trap can exert, the bead is carried away from the trap, and depending on how long the force is applied, the bead is either attracted back into the trap or escapes. The point at which the escape force was reached was measured by increasing the velocity of a triangular wave applied to one of the substage PZTs and noting when the bead position no longer reached a plateau, but instead continued to move away from the center of the trap. Escape force was found to increase linearly with laser beam power (Fig. 7), as would be expected from the previous measurements (cf. Figs. 4 *B* and 5 *B*).

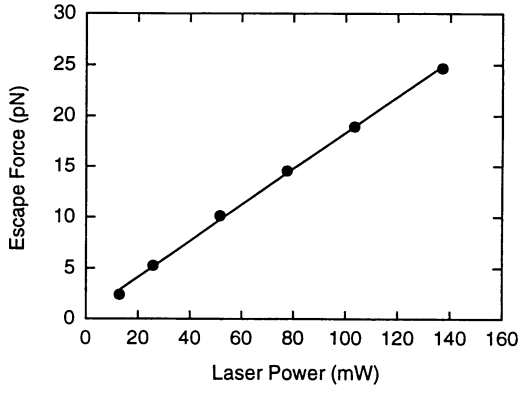

FIGURE 7 Escape force for a trapped bead (1-μm diameter) as a function of laser power. The escape force represents the maximum force an optical trap can exert to keep a bead trapped.

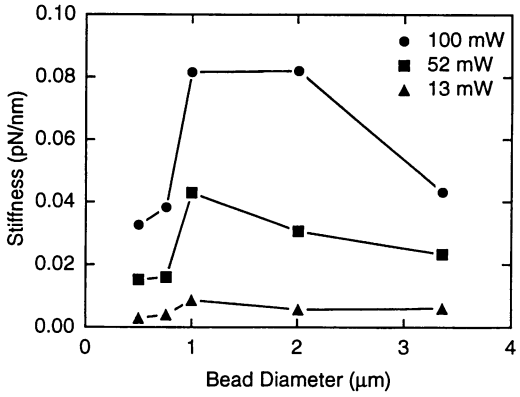

FIGURE 8 Optical trap stiffness as a function of bead diameter for laser powers of 13, 52, and 100 mW.

Measurements as a function of bead diameter

We measured the rate constants and obtained the corresponding values for the trap stiffness, k, for beads of different diameter, ranging from 0.5 to 3.36 μm. The values of k for three laser powers are plotted in Fig. 8. k increased at first with increasing bead diameter, but then reached a broad peak, probably with a maximum between 1 and 2 μm, and then declined. For beads of small diameter relative to the wavelength of the laser ($r \ll \lambda$), stiffness is expected to rise with increasing diameter, as the amount of material in the beam increases and so does the trapping power (Ashkin, 1992). On the other hand, for large particles ($r \gg \lambda$), where the ray optic regime holds, particles intercept all the converging rays at the laser focus, so the trapping force is the same, irrespective of diameter. However, the trapping rays are spread out over a larger distance the bigger the particle, so the stiffness should decrease with increasing diameter: a particle with twice the diameter has to move twice as far for the same force to be produced on it by the trap. Our results,

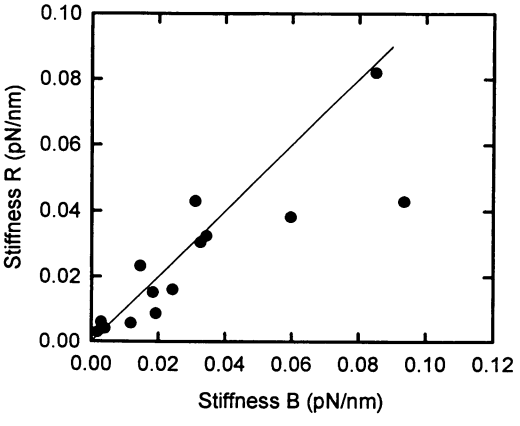

FIGURE 9 Comparison of optical trap stiffness as measured by Brownian motion (stiffness B) and by responses to rapid trap displacements (stiffness R). The line represents the ideal case, where the stiffness measurements are the same by both methods. Bead diameters ranged from 0.5 to 3.36 μm and the laser powers ranged from 13 to 100 mW.

for particles of intermediate diameter, show a peak as expected.

We also estimated stiffness by measuring the Brownian motion on the same samples, recording 50 s of data for each bead size and laser power. From the equipartition of energy, the root mean square Brownian motion along one axis, $\sqrt{x_n^2}$, is given by

$$\frac{1}{2}kx_n^2 = \frac{1}{2}k_BT,$$

where k_B is Boltzman's constant and T is the absolute temperature. Thus the stiffness, k, can be estimated; it is plotted in Fig. 9 against the stiffness calculated from the step changes of trap position. There is a good deal of scatter in the data as a result of four factors: i) for points derived from traps with a high frequency response (large rate constant), there was undoubtedly an underestimate of $\sqrt{x_n^2}$ because of the limited bandwidth of the quadrant detector (resulting from the use of large value feedback resistors needed to minimize the effects of dark noise); ii) points at a high trap stiffness had a higher proportion of instrumental noise; iii) small beads had a finite proportion of dark noise; iv) there was a substantial and variable component of low-frequency noise derived from pointing instability. We did not attempt to correct for these factors, and given the errors, Fig. 9 indicates a reasonable agreement between the two estimates of stiffness.

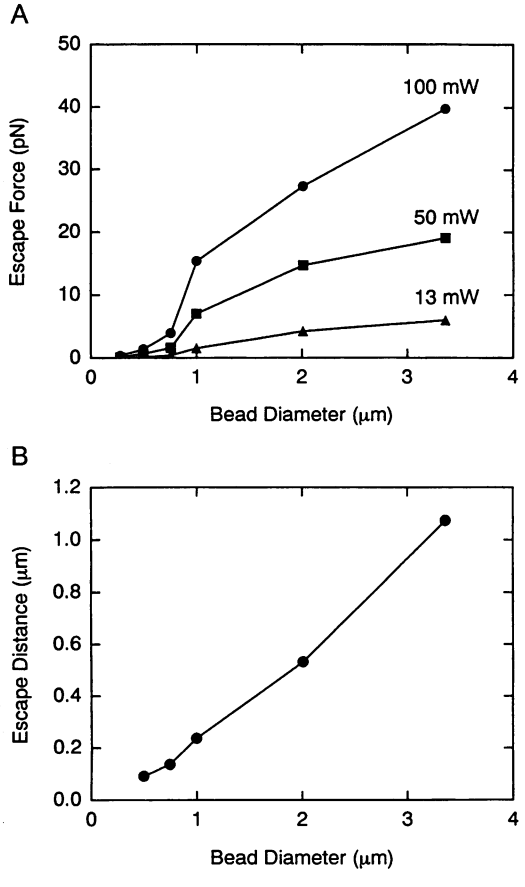

FIGURE 10 (*A*) Escape force for a trapped bead as a function of bead diameter for laser powers of 13, 52, and 100 mW. (*B*) Displacement of a trapped bead at the point of escape as a function of bead diameter for laser power of 100 mW.

Escape force was measured for beads of diameter between 0.28 and 3.36 μm. Because the escape force can be measured by visual observation of the video monitor, it was possible by using fluorescent beads to include those of diameter too small to make useful quantitative measurement of trap stiffness. Results for three laser powers are shown in Fig. 10 *A*. For a given laser power, escape force increases steeply at first with increase of bead diameter and then flattens off toward a plateau. According to Ashkin (1992), for Rayleigh particles ($r \ll \lambda$) trapping force depends on r^3, and for large particles ($r \gg \lambda$) it is independent of r. Our results, which are for sizes of particles in between these regimes, are consistent with these predictions.

For particles large enough to give displacement measurements on the quadrant detector, it was also possible to measure the escape distance, i.e., the distance the bead is displaced from the center of the trap when it escapes the force of the trap, roughly where the maximum force was observed. The values for bead diameters of 0.5–3.36 μm are plotted in Fig. 10 *B*, which shows that the escape distance lies roughly at half the radius of the bead. For 1-μm beads it would be expected that the escape distance would lie at 450 nm from the center of the trap, the value found for the maximum force in Fig. 5 *B*, but the value actually obtained was 238 nm. The reason for this discrepancy is most likely that the method used to detect the escape point results in an underestimate of the value. As the velocity of the triangular wave approaches the escape force, the bead displacement record shows a "tail," which we took at the time to be the first sign of the escape process, and noted the force and displacement just as this tail developed. It is more likely that it signifies the start of the broad peak of the profile of Fig. 5 *B*. The appearance of a tail was probably exacerbated by a slight nonlinearity of the velocity produced by the piezoelectric transducers, resulting in the Stokes' force continuing to rise somewhat during steady motion. A further factor tending to underestimate the position of the maximum of force from the escape point measurements is that the maximum represents an unstable equilibrium, and Brownian motion could help to take the bead beyond the maximum.

A linear relation between escape distance and bead size is to be expected for large particles ($r \gg \lambda$). The escape force is independent of diameter for large particles, but it is produced when a bead is displaced by approximately one diameter from the center of the trap (Ashkin, 1992). For small particles ($r \ll \lambda$), the distance from the center of the trap for the maximum force should be independent of bead size and occur where the square of the field gradient is a maximum. In this case, a rough calculation yields an escape distance on the order of 200 nm. Thus, it would be expected that as bead diameter is increased from zero, the escape distance should at first be independent of bead size, with a value of about 200 nm, and then increase as the size of bead

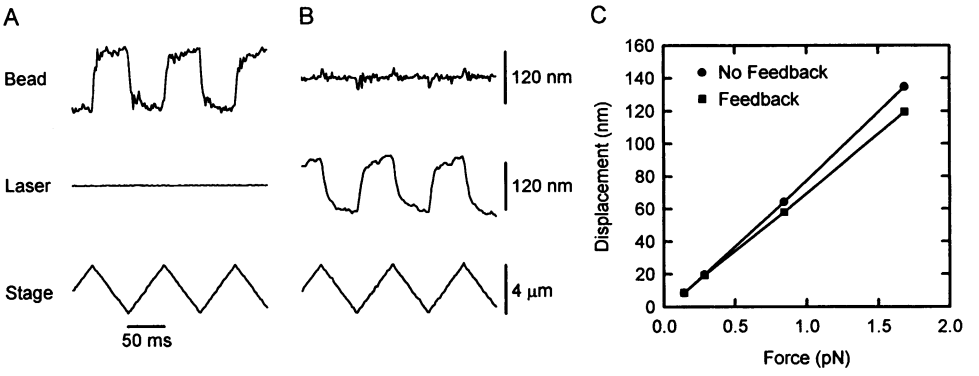

FIGURE 11 Optical trap stiffness calibration with and without feedback control. (*A*) Without feedback: the response of a trapped bead to a triangular wave input to the microscope stage position (see Fig. 6). (*B*) With feedback: the laser trap position now shows the response. (*C*) Displacement measured from bead position trace (without feedback) and from trap position trace (with feedback), as a function of applied force. Detector bandwidth was 100 Hz (single-pole, low-pass filter). Each trace is an average of 100 data sweeps.

becomes significant compared to λ, finally becoming nearly equal to the diameter (Ashkin, 1992). We were not able to measure the escape distance for beads smaller than 500 nm, but our results show the expected linear relationship as diameter increases.

Feedback control

The results so far show that the displacement of a trapped bead can be used to make time-resolved measurements of force. For measurements of small forces the trap has to be made weak enough to give detectable bead movements above the noise from Brownian motion and instrumental noise. However, this leads to a compliant measuring system, and in some applications it is desirable to make the trap at least an order of magnitude stiffer than the system under investigation to avoid perturbations. We therefore investigated the use of feedback to increase the stiffness of the trap. In feedback mode, the x_B, y_B signals from the quadrant detector are fed through amplifiers to the driver circuits for the acousto-optic modulators (Fig. 2). Ideally, when an external force is applied to a trapped bead, the position of the trap (x_T, y_T) is shifted so that the trap applies an equal and opposite force to the external force acting on the bead. As a result, the bead remains stationary and the trap movement is a measure of the external force. We made some measurements to compare the performance of the system, with and without feedback control. Fig. 11, *A* and *B*, shows records of bead and trap movement to a force applied via a triangular wave input to one of the substage piezoelectric transducers (cf. Fig. 6 *A*). The two measurements give closely similar results, showing that the feedback mode can be used to measure isometric force. Quantitative measurements of x_B, y_B without feedback and x_T, y_T with feedback confirm this (Fig. 11 *C*). We made some measurements of escape force with feedback and found that this was approximately 70% of the escape force without feedback.

It should be noted that in principle feedback can be used to stiffen a trap along a single axis; however, we found single-axis feedback to be unstable in experiments on the actomyosin motility assay (Simmons et al., 1993). Presumably the reason for the instability is that external forces on a trapped bead that pull it even slightly off axis cause bead movement at right angles, where the trap is less stiff. As a result, the two-dimensional feedback system using two orthogonal acousto-optic modulators described here offers improved stability, even when one-dimensional forces are being measured (Finer et al., 1994).

The feedback system improves the stiffness of the trap (by a factor of about 400 in the example in Fig. 11) without the need to increase the laser power. It is also highly effective at reducing the Brownian motion of a particle (compare Fig. 12, *B* and *C*), albeit at the cost of transferring the noise to the force signal. In all of the figures so far presented in this paper, the experimental data were signal averaged, and this could lead to an overoptimistic impression of the signal-to-noise ratio in single traces. Fig. 12 is included to show the noise levels at typical trap strengths used in experiments on single motor proteins, and we used an improved detector and feedback system to show the

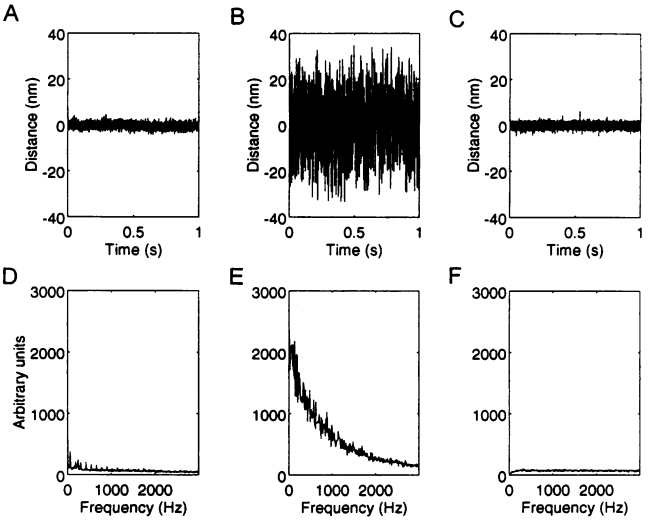

FIGURE 12 Positional noise on a 1-μm diameter bead (*A*) immobilized on a coverglass surface, (*B*) held without feedback in a laser trap with a stiffness of 0.04 pN · nm^{-1}, and (*C*) held in the same laser trap with feedback control. (*D–F*) Fourier transform spectra of the positional noise corresponding to *A–C*, respectively. Detector bandwidth was 5 kHz.

signals at full bandwidth (Inverted microscope, Materials and Methods). In motor protein experiments, displacement has to be measured at a trap stiffness that is as low as possible, typically 0.04 pN · nm^{-1} in our experiments (Finer et al., 1994). This presents a load of 0.4 pN (about 10% of the average isometric force of 3–4 pN) at a typical myosin unitary displacement of 10 nm. Fig. 12 *B* shows that the noise level at this trap stiffness is about 60 nm peak to peak (9.5 nm rms). The noise is primarily due to Brownian motion; the instrumental noise (Fig. 12 *A*) is about 3 nm peak to peak (<1 nm rms). Fig. 12 also shows the noise level when the feedback system is in operation (Fig. 12 *C*), giving a peak-to-peak noise level of about 3 nm (<1 nm rms). The corresponding noise on force was about 2.5 pN peak to peak (0.4 pN rms).

DISCUSSION

Many improvements can be made to the system described here. In preliminary work we have shown that the pointing stability of the laser can be improved by using an optical fiber, which also makes it possible to mount the laser on a separate table, thus reducing vibration. Solid-state lasers and solid-state pumped lasers also present fewer problems from vibration. Inverted microscopes offer improved stage stability compared with the upright design for most of the measurements described here. Improved efficiency and beam quality can be achieved with TeO_2 acousto-optic modulators, rather than the $PbMbO_4$ type used here. PZT-operated mirrors can also be used to deflect the laser beam provided they are servo-controlled, with adequate speed for most purposes. Detection noise can be much reduced by using a xenon arc lamp (Fig. 12), and an interferometric design offers improved performance (Denk and Webb, 1990; Svoboda et al., 1993).

Our results show that measurements of the position of a particle in an optical trap can be used to monitor external forces acting on the particle. Of particular interest to studies of biological processes is the observation that a 1-μm bead in a weak trap with feedback control can give simultaneous measurements of force and displacement with subpiconewton and nanometer resolutions, respectively, and with a response time of about 1 ms. These are in the range needed to make measurements on single molecule interactions in actomyosin and kinesin-microtubule motility assays. The main limitation on achieving these resolutions in practice lies in the noise from Brownian motion, at least if signal averaging cannot be used. In making measurements of unitary displacements, the trap stiffness must be sufficiently low that the motor protein movement is unimpeded, and this results typically in a noise of about 60 nm peak to peak (Fig. 12 *B*). Fortunately, the stiffness of the motor protein enhances the trap stiffness, and the Brownian motion noise is lowered correspondingly (Svoboda et al., 1993; Finer et al., 1994). Alternatively, it may be possible to use a somewhat higher trap stiffness (Fig. 12 *C*), if the relation between displacement and load is not steep in the region of interest (Finer et al., 1994) or the amount of displacement is constrained (Svoboda et al., 1993).

In biological experiments using trapped beads, the nature of the experiment may put limits on the size of bead to be used. However, other things being equal, the data in this paper should be useful in choosing a bead diameter to optimize stiffness, frequency response, or trap strength. In many respects, not the least being ease of detection, bigger is better, but it should be noted that both stiffness (k) and rate constant (k/b) have optimum values.

This work was supported in part by grants from the NSF and AFOSR (SC); a grant from the NIH (JAS); support from the MRC (RMS); travel grants from the Wellcome Trust and Fulbright Commission (RMS); a NATO Collaborative Research Grant (JAS, RMS); and a Human Frontier Science Program grant (JAS, SC, RMS). JTF was a trainee of the Medical Scientist Training Program at Stanford University.

REFERENCES

Ashkin, A. 1992. Forces of a single-beam gradient laser trap on a dielectric sphere in the ray optics regime. *Biophys. J.* 61:569–582.

Ashkin, A., and J. M. Dziedzic. 1977. Feedback stabilization of optically levitated particles. *Appl. Phys. Lett.* 30:202–204.

Ashkin, A., J. M. Dziedzic, J. E. Bjorkholm, and S. Chu. 1986. Observation of a single-beam gradient force optical trap for dielectric particles. *Opt. Lett.* 11:288–290.

Berns, M. W., W. H. Wright, and R. W. Steubing. 1991. Laser microbeam as a tool in cell biology. *Int. Rev. Cytol.* 129:1–44.

Block, S. M. 1990. Optical tweezers: a new tool for biophysics. *In* Noninvasive Techniques in Cell Biology. J. K. Foskett and S. Grinstein, editors. Wiley-Liss, New York. 375–402.

Denk, W., and W. W. Webb. 1990. Optical measurement of picometer displacements of transparent microscopic objects. *Appl. Opt.* 29: 2382–2391.

Finer, J. T., R. M. Simmons, and J. A. Spudich. 1994. Single myosin molecule mechanics: piconewton forces and nanometre steps. *Nature.* 368:113–119.

Happel, J., and H. Brenner. 1991. Low Reynolds Number Hydrodynamics, 2nd ed. Kluwer Academic Publishers, Dordecht, the Netherlands.

Kuo, S. C., and M. P. Sheetz. 1992. Optical tweezers in cell biology. *Trends Cell. Biol.* 2:116–118.

Kuo, S. C., and M. P. Sheetz. 1993. Force of single kinesin molecules measured with optical tweezers. *Science.* 260:232–234.

Simmons, R. M., and J. T. Finer. 1993. Glasperlenspiel II. *Curr. Biol.* 3:309–311.

Simmons, R. M., J. T. Finer, H. M. Warrick, B. Kralik, S. Chu, and J. A. Spudich. 1993. Force on single actin filaments in a motility assay measured with an optical trap. *In* Mechanism of Myofilament Sliding in Muscle. H. Sugi and G. H. J. Pollock, editors. Plenum, New York, London. 331–336.

Svoboda, K., and S. M. Block. 1994. Biological applications of optical forces. *Annu. Rev. Biophys. Biomol. Struct.* 23:247–285.

Svoboda, K., C. F. Schmidt, B. J. Schnapp, and S. M. Block. 1993. Direct observation of kinesin stepping by optical trapping interferometry. *Nature.* 365:721–727.